GEOPHYSICAL RESEARCH LETTERS, VOL. 40, 5944–5948, doi:10.1002/2013GL058118, 2013

Robust increase in equilibrium climate sensitivity under global warming

Katharina Meraner,[1] Thorsten Mauritsen,[1] and Aiko Voigt[1,2]

Received 27 September 2013; revised 5 November 2013; accepted 5 November 2013.

[1] Equilibrium climate sensitivity (ECS) is a widely accepted measure of Earth's susceptibility to radiative forcing. While ECS is often assumed to be constant to a first order of approximation, recent studies suggested that ECS might depend on the climate state. Here it is shown that the latest generation of climate models consistently exhibits an increasing ECS in warmer climates due to a strengthening of the water-vapor feedback with increasing surface temperatures. The increasing ECS is replicated by a one-dimensional radiative-convective equilibrium model, which further shows that the enhanced water-vapor feedback follows from the rising of the tropopause in a warming climate. This mechanism is potentially important for understanding both warm climates of Earth's past and projections of future high-emission scenarios. **Citation:** Meraner, K., T. Mauritsen, and A. Voigt (2013), Robust increase in equilibrium climate sensitivity under global warming, *Geophys. Res. Lett.*, *40*, doi:10.1002/2013GL058118.

1. Introduction

[2] Equilibrium climate sensitivity (ECS) is defined as the change in the global mean surface temperature after reaching equilibrium in response to a doubling of the atmospheric CO_2 concentration [*Randall et al.*, 2007]. The concept of ECS has its origin in the work of *Arrhenius* [1896], who more than a century ago showed that radiative forcing from CO_2 is an approximately logarithmic function of the atmospheric concentration. Indeed, if the radiative response of the climate system was linear, then the equilibrium temperature response to any CO_2 doubling will be constant regardless of the starting point. The extent to which the assumptions of state-independent forcing and linear radiative response apply is, however, a matter of ongoing debate [e.g., *Hansen et al.*, 2005; *Colman and McAvaney*, 2009; *Caballero and Huber*, 2010; *Jonko et al.*, 2012; *Caballero and Huber*, 2013].

[1]Max Planck Institute for Meteorology, Hamburg, Germany.
[2]Laboratoire de Meteorologie Dynamique, IPSL, Universite Pierre et Marie Curie, Paris, France.

Corresponding author: K. Meraner, Max Planck Institute for Meteorology, Bundesstrasse 53, 20146 Hamburg, Germany. (katharina.meraner@mpimet.mpg.de.)

0094-8276/13/10.1002/2013GL058118

[3] To appreciate the problem, consider Earth's energy balance in response to a doubling of CO_2,

$$\Delta R = F + \lambda \Delta T, \tag{1}$$

where F is the radiative forcing due to the CO_2 doubling and ΔR the resulting imbalance in the top-of-atmosphere radiation. $\lambda \Delta T$ describes the radiative response of the climate system and is written as the product of the temperature change ΔT with respect to a base state and the system's total feedback, λ. It is common practice to decompose λ into contributions from temperature (λ_T), water vapor (λ_W), clouds (λ_C), and surface albedo (λ_A). While λ itself has to be negative to yield a stable climate, its individual contributions can be positive (e.g., λ_W) or negative (e.g., λ_T). Within this framework, the temperature change after the climate system has reached equilibrium again ($\Delta R = 0$) defines the value of ECS = $-F/\lambda$. Consequently, an increase in ECS can arise from either an enhanced forcing, a positive change in the feedback, or both.

[4] The issue of a possible increase of ECS in warmer climates recently received attention in several single-model studies, though these studies yielded conflicting results. *Colman and McAvaney* [2009] successively doubled CO_2 from $\frac{1}{16}$ to 32 times the present-day CO_2 concentration in the BMRC atmospheric model and found that an increase in CO_2 forcing was approximately compensated by a negative change in the feedback in warmer climates. As a result, the Bureau of Meteorology Research Center (BMRC) model exhibited a slightly decreasing ECS. A similar effect was found earlier by *Manabe and Bryan* [1985] in the Geophysical Fluid Dynamics Laboratory (GFDL) model. Both studies suggested that the negative change in the feedback stemmed primarily from a diminishing surface albedo feedback in warmer climates. Contrary to these, studies based on the National Center for Atmospheric Research (NCAR) climate models found an increasing ECS in warmer climates [*Caballero and Huber*, 2010; *Jonko et al.*, 2012; *Caballero and Huber*, 2013], whereas the Goddard Institute for Space Studies (GISS) model exhibits a minimum ECS around present-day conditions and higher ECS in both colder and warmer climates [*Hansen et al.*, 2005].

[5] The fifth phase of the Coupled Model Intercomparison Project (CMIP5) includes a coupled model experiment with abruptly quadrupled CO_2. This experiment is designed to estimate ECS through a regression of the radiation imbalance on surface temperature change [*Gregory et al.*, 2004]. The feedback (λ) equals the slope of the regression line. The majority of CMIP5 coupled models exhibit nonlinearity in this experiment, with a steeper slope ($\approx \lambda$) in the first decades, corresponding to a smaller effective ECS, followed by a weaker slope, corresponding to a higher effective ECS.

Table 1. Global Surface Temperature Changes ΔT [K] With Respect to the Preindustrial Control Simulation, Equilibrium Climate Sensitivities ECS [K], Adjusted Forcings F [Wm^{-2}], and Total Feedbacks λ [$Wm^{-2}\,K^{-1}$] for the ECHAM6 Mixed-Layer Ocean Experiments[a]

	2×CO_2	4×CO_2	8×CO_2	16×CO_2
ΔT	2.79 ± 0.04	6.70 ± 0.04	12.46 ± 0.07	22.68 ± 0.11
ECS	2.79 ± 0.04	3.91 ± 0.06	5.76 ± 0.08	10.22 ± 0.13
F	4.26 ± 0.20	4.83 ± 0.30	5.15 ± 0.79	4.94 ± 1.06
λ_T	–4.27 ± 0.02	–4.11 ± 0.01	–4.30 ± 0.00	–4.28 ± 0.00
λ_W	2.12 ± 0.01	2.14 ± 0.01	2.48 ± 0.00	2.78 ± 0.01
λ_C	0.32 ± 0.03	0.36 ± 0.01	0.59 ± 0.01	0.66 ± 0.00
λ_A	0.17 ± 0.00	0.21 ± 0.00	0.11 ± 0.00	0.06 ± 0.00
$\sum \lambda_i$	–1.63 ± 0.06	–1.36 ± 0.03	–1.05 ± 0.02	–0.74 ± 0.01
λ	–1.65 ± 0.04	–1.35 ± 0.01	–1.03 ± 0.01	–0.67 ± 0.01

[a] λ is further decomposed by the PRP method into contributions from temperature (T), water vapor (W), clouds (C) and surface albedo (A). The uncertainties for λ correspond to the 95% confidence intervals of the regression. For ΔT and ECS, we use the last 20 years of the mixed-layer ocean simulations to calculate the standard errors of ΔT and ECS. The uncertainty of ΔT and ECS is then given by two times the standard error. For F, the uncertainty is measured by two times the standard error of F in the fixed SST simulations. All changes are found to be statistically significant compared to the 2×CO_2 values, except the adjusted forcing of the 16×CO_2 simulation.

The leading hypothesis is that this nonlinearity is related to the spatial distribution of surface warming which is initially dampened at high latitudes due to regional ocean heat uptake [*Winton et al.*, 2010]. Because the local feedback at higher latitudes is typically less negative than the global feedback, or even positive, this could explain the time-varying slope [*Armour et al.*, 2013]. It is, however, difficult to distinguish this adjustment process from a state dependence of the feedback and its individual contributions [*Block and Mauritsen*, 2013]. Furthermore, it remains unclear whether the regression method is representative of the long-term equilibrium response [*Li et al.*, 2013].

[6] Motivated by these previous studies, this contribution evaluates ECS across a hierarchy of models ranging from fully coupled contemporary climate models of CMIP5, one of which we analyze in detail coupled to a mixed-layer ocean, down to an idealized one-dimensional radiative-convective equilibrium model. Across these models we find a robust increase of ECS in warmer climates due to a strengthening of the water-vapor feedback.

2. Data and Methods

[7] We use climate model output from the following three CMIP5 experiments: preindustrial control simulations (piControl), simulations with instantaneously quadrupled atmospheric CO_2 concentration (abrupt4×CO_2), and the extended Representative Concentration Pathway 8.5 future scenario (RCP8.5). The latter is a scenario without mitigation; however, in the present study we simply utilize the fact that the experiment protocol prescribes constant greenhouse gases from year 2249 to 2300 including CO_2 at 1962 ppm. This permits a regression of ΔR against ΔT to estimate λ using equation (1) at relatively warm temperatures [*Gregory et al.*, 2004]. The 95% confidence intervals of λ are calculated assuming normally distributed regression errors and using the 0.975 percentile of Student's t distribution with the appropriate degrees of freedom. Properties of two simulations are considered statistically significantly different if the 95% confidence interval of the warmer simulation is distinct from the mean value of the colder simulation. Six models, MPI-ESM-LR [*Giorgetta et al.*, 2013], IPSL-CM5A-LR [*Hourdin et al.*, 2013], HadGEM2-ES [*Collins et al.*, 2008], CSIRO-Mk3.6.0 [*Gordon et al.*, 2002], CNRM-CM5 [*Voldoire et al.*, 2013], and BCC-CSM1.1 [*Wu et al.*, 2010] provide the necessary data for the analysis. One realization is used from all experiments as only one model provided multiple realizations of the extended RCP8.5 experiment.

[8] The atmospheric component of the MPI-ESM-LR coupled model is ECHAM6 (Version 6.1) at T63 horizontal spectral resolution with 47 vertical levels, including a representation of the stratosphere with the uppermost level at 0.01 hPa, or about 80 km [*Stevens et al.*, 2013]. Here ECHAM6 is coupled to a 50 m mixed-layer ocean with prescribed ocean energy transport (q flux) that we derive from a 30 year Atmospheric Model Intercomparison Project simulation with observed sea-surface temperatures and sea ice from the past three decades. In addition to a control simulation, the model is forced by abruptly applying 2, 4, 8, and 16 times preindustrial CO_2 (284.7 ppm). All simulations are 50 years long. In these simulations we evaluate individual feedbacks due to water vapor, temperature, clouds, and surface albedo by means of the partial radiative perturbation (PRP) method [*Wetherald and Manabe*, 1988; *Colman and McAvaney*, 1997]. We apply a 10-hourly subsampling of instantaneous model fields such that a full diurnal cycle is sampled over 5 days. The PRP calculations are performed throughout the 50 year simulations permitting an evaluation of feedbacks by regressing individual flux contributions on global mean temperature [*Colman and McAvaney*, 2011]. This technique yields an elegant separation between fast adjustments directly caused by the CO_2 increase, which in ECHAM6 are primarily stratospheric adjustment and a fast cloud reduction, and true surface temperature-dependent feedbacks that are realized subsequently [*Block and Mauritsen*, 2013]. For instance, it is not necessary to distinguish between the troposphere and stratosphere when evaluating the temperature feedback, which is particularly important for the 16×CO_2 run that exhibits a rise of the tropical tropopause to about 30 km. The methodology is thus directly applicable to the nonlinear regime, as opposed to the widely used radiative kernel technique [*Soden et al.*, 2008; *Jonko et al.*, 2012]. The method yields negligible systematic errors, evidenced by small differences between $\sum \lambda_i$ and λ in Table 1. Adjusted forcing is determined from runs with prescribed sea-surface temperatures and increased CO_2, corrected for the small global mean surface temperature change due to land warming [*Hansen et al.*, 2005].

3. Results

[9] We compare total feedbacks (λ) as the slope of the regression line derived from the abrupt4×CO_2 runs with those derived from the end of the warmer extended RCP8.5 run to investigate to what extent ECS of the coupled CMIP5 models depends on the base state. Indeed, four out of the six models exhibit a statistically significant positive change in λ in the extended RCP8.5 experiment relative to the abrupt4×CO_2 at the 95% confidence level, as can be inferred from the fact that the regression lines are more flat in RCP8.5 (Figure 1). This positive change implies an increased ECS in the RCP8.5 runs compared to the abrupt4×CO_2 runs. Most

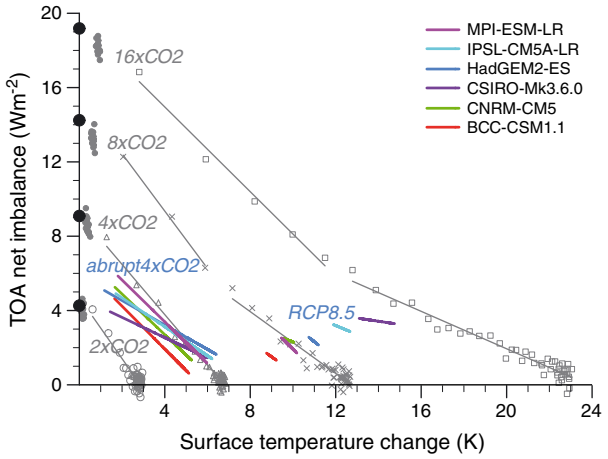

Figure 1. Gregory plot for the ECHAM6 mixed-layer ocean experiments ($2\times CO_2$, $4\times CO_2$, $8\times CO_2$, and $16\times CO_2$; gray regression lines and symbols) and abrupt$4\times CO_2$ and RCP8.5 experiments of the CMIP5 models (colored lines). For the RCP8.5 experiment regressions are shown for the last part of the extended scenarios for which all externally prescribed greenhouse gases are held constant. The black filled circles depict the adjusted forcing for the ECHAM6 mixed-layer ocean experiments. The adjusted forcing is calculated by fixed sea-surface temperature experiments (gray filled circles show individual years) and correcting for small changes in land temperatures.

notably, λ of CSIRO-Mk3.6.0 in RCP8.5 is only weakly negative, indicating that this particular model is close to a runaway for which further surface warming hardly reduces the reduced radiation imbalance. HadGEM2-ES exhibits a statistically significant negative change in λ in the warmer climate, whereas for MPI-ESM-LR λ is statistically indistinguishable between the two experiments.

[10] Interestingly, despite not being statistically detectable in MPI-ESM-LR runs, we find a distinct positive change in λ and corresponding rise in ECS in warmer climates in experiments conducted with its atmospheric component model, ECHAM6, coupled to a mixed-layer ocean (gray lines and symbols in Figure 1 and column 1 in Table 1). For the fourth doubling of CO_2 the model's ECS exceeds 10 K, measured between equilibrium states of $8\times CO_2$ and $16\times CO_2$, as opposed to less than 3 K for the first doubling of CO_2 over preindustrial (Figure 1 and Table 1). The model exhibits a slight increase in adjusted forcing in warmer climates (column 3 in Table 1); however, the rise in forcing is not sufficient to explain the rise in ECS. Hence, the rise in ECS in this model is due mainly to a positive change of λ in warmer climates, which is evident from the weakening slopes in Figure 1.

[11] Inspecting the change in the individual longwave and shortwave components of the top-of-atmosphere irradiance, a positive slope in Figure 2 contributes to an increasing climate sensitivity and represents a positive change in the corresponding feedback (vice versa for negative slopes). With only one exception (BCC-CSM1.1), there is a positive change in both the longwave all-sky and clear-sky feedback in the warmer RCP8.5 relative to the abrupt4×CO2 simulations (positive red and blue slopes in Figure 2). Likewise, the mixed-layer ocean runs with ECHAM6 show progressively positive changes in the longwave feedback in warmer climates (positive gray slopes at the bottom of Figure 2), which is primarily attributable to an increase in the water-vapor feedback (Table 1). The temperature feedback remains nearly constant, whereas the cloud feedback rises in ECHAM6. In the shortwave, the CMIP5 models consistently exhibit a negative change of the clear-sky feedback (negative green slopes in Figure 2), likely associated with the vanishing perennial sea ice at the warm temperatures in RCP8.5. This effect alone would decrease the ECS, but the all-sky shortwave feedback, which includes the effect of clouds, is nearly constant in the ensemble mean, despite substantial intermodel spread. It is noteworthy that in the shortwave, the CSIRO-Mk3.6.0 model sticks out from the ensemble with the largest positive all-sky feedback (top purple line in Figure 2), indicating that cloud feedback is likely the cause of the near-runaway warming of that model in the RCP8.5 experiment (Figure 1). Overall, however, the strong variability in changes of the shortwave feedback indicates that these changes cannot play a dominant role in the rise of ECS in the CMIP5 model ensemble.

[12] Instead, the rise in ECS is consistently rooted in a positive change of the longwave feedback (Figure 3). The local longwave feedback, defined as the grid point-wise increase in outgoing longwave radiation per local degree warming, reveals that in the ensemble mean the rise occurs almost exclusively in the tropics between 30°S and 30°N, whereas midlatitudes and high latitudes counteract (Figure 3). The same pattern is found in clear-sky fluxes (not shown). Even though an increased poleward energy transport could contribute to this pattern, it does suggest that an enhanced tropical water-vapor feedback is the main cause of the rise in ECS in the CMIP5 models.

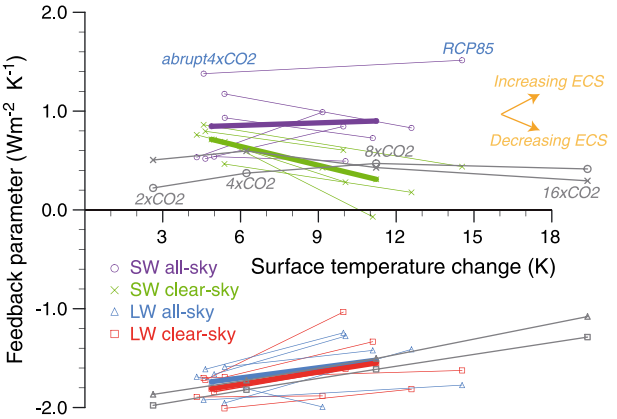

Figure 2. Trend in the values of the shortwave, longwave, clear-sky, and all-sky feedback between the abrupt$4\times CO_2$ and extended RCP8.5 simulations of CMIP5 (colored lines) and between the different CO_2 simulations with ECHAM6 (gray lines). Feedbacks are calculated using the Gregory method. For each feedback, a line connects its values for the different simulations to indicate if the feedback undergoes a positive or negative change with increasing surface temperature. A positive slope represents a contribution to increasing ECS, whereas a negative slope is a contribution to a decrease in ECS (cf. the orange arrows). Bold colored lines represent the ensemble mean for CMIP5 models.

4. Radiative-Convective Model of Tropical Water-Vapor Feedback

[13] To understand whether the local tropical water-vapor feedback can indeed account for the rise in ECS, we use an idealized one-dimensional radiative-convective equilibrium model (RCE model). The RCE model is helpful to understand tropical feedbacks as the tropics are close to radiative-convective equilibrium [e.g., *Popke et al.*, 2013] and different variants of RCE models have long been central to our understanding of the water-vapor feedback [e.g., *Manabe and Strickler*, 1964; *Stevens and Bony*, 2013]. We apply a diagnostic framework similar to that used by *Kasting* [1988] to study a runaway greenhouse. In the RCE model, temperature in the troposphere follows a moist adiabat, relative humidity is held fixed at 80%, and the stratosphere has a constant temperature and humidity equal to that at the tropopause. In accordance with the fixed anvil temperature hypothesis of *Hartmann and Larson* [2002] and a rise of the tropopause height in warmer climates [*O'Gorman and Singh*, 2013], the tropopause temperature is fixed at 200 K. Only longwave radiative transfer [*Fu and Liou*, 1993] is considered. λ is calculated from the increase in outgoing longwave radiation at the top of the atmosphere per degree surface warming. With this setup, ECS $= -F/\lambda$, where $F = 4\ \mathrm{Wm^{-2}}$ approximately equals the radiative forcing from a doubling of CO_2. The conclusions drawn based on this model are independent of parametric choices within a reasonable range.

[14] The RCE model exhibits a distinct rise in ECS from about 2 K at cold surface temperatures to 6 K around 40°C (black line in Figure 4). The rise in ECS results from an enhanced (i.e., more positive) water-vapor feedback, as can be inferred from difference to a corresponding system without water-vapor feedback (green line in Figure 4). The qualitative agreement with ECHAM6 in the range of the $2\times CO_2$ and $8\times CO_2$ experiments is striking, despite the immense gap in complexity between the two models. When instead the RCE model is run with a fixed tropopause pressure of 200 hPa, ECS drops from about 2 K to less than 1 K at warm temperatures. Thus, the rising of the tropopause appears crucial to the increase in ECS.

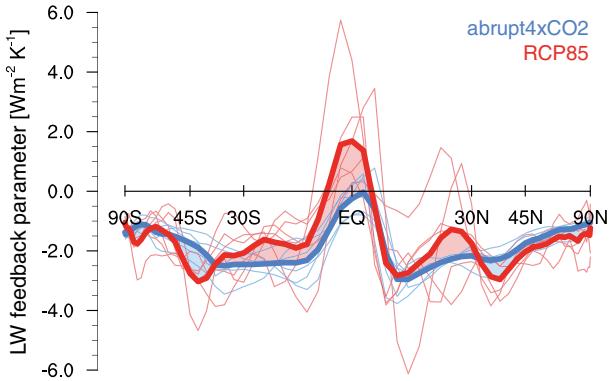

Figure 3. Zonal average local longwave all-sky feedback for the six CMIP5 models for abrupt4×CO_2 (blue lines) and RCP8.5 (red lines). Thick lines represent ensemble means. The local feedback is calculated by regressing the local longwave all-sky radiative flux change against the local surface temperature change. Red shading indicates areas where the local feedback becomes more positive from abrupt4×CO_2 to RCP8.5. The feedback becomes more negative in regions with blue shading.

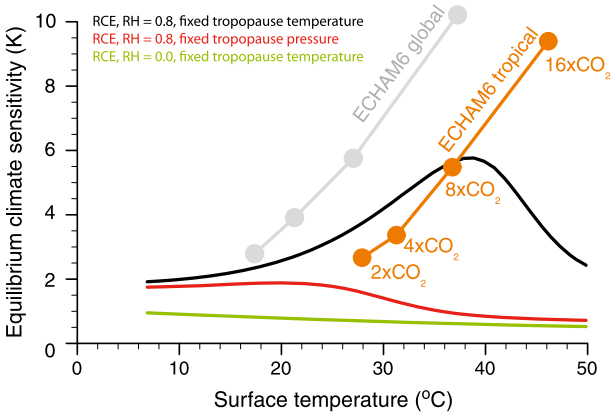

Figure 4. Equilibrium climate sensitivity of the RCE model with relative humidity (RH) fixed assuming either a fixed tropopause temperature (black line) or a fixed tropopause pressure (red line) as a function of surface temperature. Also shown is the case with fixed tropopause temperature but without water-vapor feedback (green line). Global and tropical equilibrium climate sensitivities of the ECHAM6 model coupled to a mixed-layer ocean are shown in gray and orange, respectively.

[15] The ECS decreases in the RCE model for surface temperatures above 40°C because the moist adiabat becomes increasingly steep and the amount of mass in the cold tropopause region diminishes. This weakens the water-vapor feedback relative to temperature feedback at very high temperatures and results in a decreasing ECS. This effect does not seem to be dominant in ECHAM6 for reasons that are not yet fully understood.

5. Conclusions

[16] We investigate the extent to which equilibrium climate sensitivity (ECS) depends on the climate base state. To this end, we evaluate a hierarchy of models ranging from contemporary global climate models that include the dynamics of the atmosphere and ocean to a one-dimensional radiative-convective equilibrium model. Across these models we find a systematic positive change in the feedback (λ) toward less negative values, resulting in an increase in ECS in warmer climates. The increase in ECS is consistently rooted in an intensification of the water-vapor feedback, which we attribute to a rise in the tropopause height by means of a radiative-convective equilibrium model. A rising tropopause is a robust feature of climate models [*O'Gorman and Singh*, 2013], dictated by thermal emission from water vapor becoming less important below a temperature of about 200 K [*Hartmann and Larson*, 2002].

[17] In fact, an increase in ECS in warmer climates not only occurs in the set of models investigated here but was previously reported in the GISS model [*Hansen et al.*, 2005] and in both the coupled and mixed-layer ocean model versions of the NCAR model [*Caballero and Huber*, 2010; *Jonko et al.*, 2012; *Caballero and Huber*, 2013]. While some studies reported no rise in ECS in warmer climates [*Manabe and Bryan*, 1985; *Colman and McAvaney*, 2009],

it is noteworthy that the later studies applied models with relatively low vertical resolutions, which may hinder a faithful representation of the rising tropopause. However, we cannot exclude that other reasons might explain the decrease in ECS in these models; in particular the cloud feedback has the potential to alter the behavior. There are further strong arguments also for an increased ECS in colder climates due to enhanced surface albedo feedback [*Kutzbach et al.*, 2013], although data-based estimates of the climate sensitivity during the Last Glacial Maximum favor a lower sensitivity [*Rohling et al.*, 2012].

[18] The available evidence suggests that climate sensitivity depends considerably on the reference climate state. This has important implications for attempts to estimate ECS from paleoclimate data [*Crucifix*, 2006; *Rohling et al.*, 2012]. In particular, estimates of the ECS from climates much warmer than today, such as the Paleocene-Eocene, would naturally yield higher values than studies based on observed recent climate change [e.g., *Otto et al.*, 2013]. The latter, in turn, may not be representative for projecting future high-emission climate scenarios, and so understanding the fundamental physics underlying a possible rise in climate sensitivity in warmer climates is of value and should be more systematically explored in future climate model intercomparisons.

[19] **Acknowledgments.** The authors acknowledge scientific and practical input from Malte Heinemann, Hauke Schmidt, Bjorn Stevens, Karoline Block, Alexandra Jonko, Ray Pierrehumbert, Rodrigo Caballero, Jonas Nycander, and Florian Rauser among others. This study was supported by the Max-Planck-Gesellschaft (MPG), funding through the EUCLIPSE project from the European Union, and Seventh Framework Programme (FP7/2007-2013) under grant agreement 244067, and computational resources were made available by Deutsches Klimarechenzentrum (DKRZ) through support from Bundesministerium für Bildung und Forschung (BMBF). Aiko Voigt acknowledges support from the German Science Foundation under grant agreement VO 1765/3-1.

[20] The Editor thanks two anonymous reviewers for their assistance in evaluating this paper.

References

Armour, K., C. M. Bitz, and G. H. Roe (2013), Time-varying climate sensitivity from regional feedbacks, *J. Clim.*, *26*, 4518–4534, doi:10.1175/JCLI-D-12-00544.1.

Arrhenius, S. (1896), On the influence of carbonic acid in the air upon the temperature of the ground, *Philos. Mag. J. Sci.*, *41*(5), 237–276.

Block, K., and T. Mauritsen (2013), Forcing and feedbacks in the MPI-ESM-LR coupled model under abruptly quadrupled CO_2, *J. Adv. Model. Earth Syst.*, *5*, 1–16, doi:10.1002/jame.20041.

Caballero, R., and M. Huber (2010), Spontaneous transition to superrotation in warm climates simulated by CAM3, *Geophys. Res. Lett.*, *37*(11), L11701, doi:10.1029/2010GL043468.

Caballero, R., and M. Huber (2013), Evolving climate sensitivity: Implications of feedback analysis of early Paleogene simulations, *PNAS*, *110*(35), 14,162–14,167, doi:10.1073/pnas.1303365110.

Collins, W. J., et al. (2008), Evaluation of the HadGEM2 model, *Report 74,* Met Office Hadley Centre, Exeter, U. K.

Colman, R.-A., and B. McAvaney (2009), Climate feedbacks under a very broad range of forcing, *Geophys. Res. Lett.*, *36*, L01702, doi:10.1029/2008GL036268.

Colman, R. A., and B. J. McAvaney (1997), A study of general circulation model climate feedbacks determined from perturbed sea surface temperature experiments, *J. Geophys. Res.*, *102*(D16), 19,383–19,402, doi:10.1029/97JD00206.

Colman, R. A., and B. J. McAvaney (2011), On tropospheric adjustment to forcing and climate feedbacks, *Clim. Dyn.*, *36*, 1649–1658, doi:10.1007/s00382-011-1067-4.

Crucifix, M. (2006), Does the Last Glacial Maximum constrain climate sensitivity?, *Geophys. Res. Lett.*, *33*(18), L18701, doi:10.1029/2006GL027137.

Fu, Q., and K. N. Liou (1993), Parameterization of the radiative properties of cirrus clouds, *J. Atmos. Sci.*, *50*(13), 2008–2025.

Giorgetta, M. A., et al. (2013), Climate and carbon cycle changes from 1850 to 2100 in MPI-ESM simulations for the Coupled Model Intercomparison Project Phase 5, *J. Adv. Model. Earth Syst.*, *5*, 572–597, doi:10.1002/jame.20038.

Gordon, H. B., et al. (2002), The CSIRO Mk3 climate system model, *Report 60,* CSIRO Atmospheric Research, Aspendale.

Gregory, J. M., W. J. Ingram, M. A. Palmer, G. S. Jones, P. A. Stott, R. B. Thorpe, J. A. Lowe, T. C. Johns, and K. D. Williams (2004), A new method for diagnosing radiative forcing and climate sensitivity, *Geophys. Res. Lett.*, *31*(3), L03205, doi:10.1029/2003GL018747.

Hansen, J., et al. (2005), Efficacy of climate forcings, *J. Geophys. Res.*, *110*, D18104, doi:10.1029/2005JD005776.

Hartmann, D. L., and K. Larson (2002), An important constraint on tropical cloud–climate feedback, *Geophys. Res. Lett.*, *29*(20), 1951, doi:10.1029/2002GL015835.

Hourdin, F., et al. (2013), Impact of the LMDZ atmospheric grid configuration on the climate and sensitivity of the IPSL-CM5A coupled model, *Clim. Dyn.*, *40*(9-10), 2167–2192, doi:10.1007/s00382-012-1411-3.

Jonko, A. K., K. M. Shell, B. M. Sanderson, and G. Danabasoglu (2012), Climate feedbacks in CCSM3 under changing CO_2 forcing. Part II: Variation of climate feedbacks and sensitivity with forcing, *J. Clim.*, *26*, 2784–2795, doi:10.1175/JCLI-D-12-00479.1.

Kasting, J. F. (1988), Runaway and moist greenhouse atmospheres and the evolution of Earth and Venus, *Icarus*, *74*, 472–494, doi:10.1016/0019-1035(88)90116-9.

Kutzbach, J. E., F. He, S. J. Vavrus, and W. F. Ruddiman (2013), The dependence of equilibrium climate sensitivity on climate state: Applications to studies of climates colder than present, *Geophysical Research Letters*, *40*, 3721–3726, doi:10.1002/grl.50724.

Li, C., J.-S. von Storch, and J. Marotzke (2013), Deep-ocean heat uptake and equilibrium climate response, *Clim. Dyn.*, *40*, 1071–1086, doi:10.1007/s00382-012-1350-z.

Manabe, S., and K. Bryan (1985), CO2-induced change in a coupled ocean-atmosphere model and its paleoclimatic implications, *J. Geophys. Res.*, *90*, 1689–1707, doi:10.1029/JC090iC06p11689.

Manabe, S., and R. F. Strickler (1964), Thermal equilibrium of the atmosphere with a convective adjustment, *J. Atmos. Sci.*, *21*(4), 361–385.

O'Gorman, P. A., and M. S. Singh (2013), Vertical structure of warming consistent with an upward shift in the middle and upper troposphere, *Geophys. Res. Lett.*, *40*(9), 1838–1842, doi:10.1002/grl.50328.

Otto, A., et al. (2013), Energy budget constraints on climate response, *Nat. Geosci.*, *6*, 415–416, doi:10.1038/ngeo1836.

Popke, D., B. Stevens, and A. Voice (2013), Climate and climate change in a radiative-convective equilibrium version of ECHAM6, *J. Adv. Model. Earth Syst.*, *5*(1), 1–14, doi:10.1029/2012MS000191.

Randall, D., et al. (2007), Climate models and their evaluation, in *Climate Change 2007: The Physical Science Basis. Contribution of Working Group I to the Fourth Assessment Report of the Intergovernmental Panel on Climate Change*, edited by S. Solomon et al., pp. 589–662, Cambridge Univ. Press, Cambridge, U. K.

Rohling, E. J., et al. (2012), Making sense of palaeoclimate sensitivity, *Nature*, *491*(7426), 683–691, doi:10.1038/nature11574.

Soden, B. J., I. M. Held, R. Colman, K. M. Shell, J. T. Kiehl, and C. A. Shields (2008), Quantifying climate feedbacks using radiative kernels, *J. Climate*, *21*(14), 3504–3520, doi:10.1175/2007JCLI2110.1.

Stevens, B., and S. Bony (2013), Water in the atmosphere, *Phys. Today*, *66*(6), 29–34, doi:10.1063/PT.3.2009.

Stevens, B., et al. (2013), The atmospheric component of the MPI-M Earth system model: ECHAM6, *J. Adv. Model. Earth Syst.*, *5*, 146–172, doi:10.1002/jame.20015.

Voldoire, A., et al. (2013), The CNRM-CM5.1 global climate model: Description and basic evaluation, *Clim. Dyn.*, *40*, 2091–2121, doi:10.1007/s00382-011-1259-y.

Wetherald, R. T., and S. Manabe (1988), Cloud feedback processes in a general circulation model, *J. Atmos. Sci.*, *45*(8), 1397–1416.

Winton, M., K. Takahashi, and I. M. Held (2010), Importance of ocean heat uptake efficacy to transient climate change, *J. Clim.*, *23*, 2333–2344, doi:10.1175/2009JCLI3139.1.

Wu, T., R. Yu, F. Zhang, Z. Wang, M. Dong, L. Wang, X. Jin, D. Chen, and L. Li (2010), The Beijing climate center atmospheric general circulation model: Description and its performance for the present-day climate, *Clim. Dyn.*, *34*(1), 123–147.